Boundary-Value Problem for Magnetoelastic Waves in a Metallic Film

M. H. SEAVEY, JR.

Air Force Cambridge Research Laboratories, L. G. Hanscom Field, Bedford, Massachusetts

(Received 27 November 1967)

A boundary-value problem using traveling-wave magnetoelastic normal modes is solved for the case of a ferromagnetic metal film attached to a substrate. A specialization is made to certain spin-wave resonance experiments in the vicinity of 57.8 GHz, reported recently by Weber. For the dc magnetic field perpendicular to the plane of the film, the general dispersion relation for coupled electromagnetic, spin-wave, and acoustic modes is described. The effect of damping on the shape of the dispersion curves is discussed. For the choice of conductivity, the eddy-current exchange effects in the magnetoelastic crossover region are shown to be small. An expression for the power absorption by the film as a function of dc magnetic field is calculated assuming that the spins are pinned on the film surfaces. The magnetic field shift of a particular spin-wave resonance peak as a function of frequency through magnetoelastic crossover is computed. Values of the magnetoelastic constant b and the phenomenological phonon relaxation time τ obtained by Weber are adjusted slightly to take into account the effect of the glass substrate: b is decreased from 6.87×10^7 to 6.66×10^7 erg/cm^3, and τ is increased from 0.90×10^{-10} to 1.00×10^{-10} sec.

INTRODUCTION

THE observation of a magnon-phonon interaction in spin-wave resonance (SWR) by Weber[1] (referred to as W) constitutes the first evidence of plane magnetoelastic waves[2–5] of well-defined frequency and wave number in a ferromagnetic metal film. Previous work,[6–12] concerned with acoustic wave generation and detection by the films, has invoked magnetic inhomogeneities[10–12] and/or surface effects[6–9] to interpret observed results—a single magnetoelastic crossover frequency could not be identified. A basic reason for this, in addition to the fact that some of the films had inhomogeneous magnetization, was that the acoustic wavelength at the frequencies used (≈ 9 GHz) was of the order of the film thickness. The diagonalization procedure for the Hamiltonian containing a one-magnon–one-phonon term, valid for a bulk crystal, is no longer applicable when the inverse film thickness is comparable to the magnon or phonon k number.[13] Thus plane magnetoelastic waves, which would be expected only if the above diagonalization were allowed, are unlikely to be found at such frequencies in the thin films. At the frequency (≈ 60 GHz) of the W experi-

ment, however, the wavelength of the degenerate spin waves and phonons is less than $\frac{1}{10}$ of the film thickness (≈ 6000 Å). Thus the bulk theory is expected to be a good approximation and magnetoelastic waves become good normal modes of the system.

In the present paper use is made of the traveling-wave magnetoelastic normal modes to solve a boundary-value problem for the film attached to a substrate.[14] This treatment differs from that used in W, where the analysis initially uses superpositions of characteristic functions to represent the spin wave and acoustic wave in the film.[15] Curves of the magnetic field shift of a given SWR as a function of frequency in the crossover region are obtained. The numerical treatment is confined to one of the experimental cases in W. The SWR tuning curve obtained here agrees closely with the prediction of W for the case of the substrate-free film, and in turn the prediction of W fits his experimental points except on the two wings of the curve. In the presence of the substrate the values of τ and b, the phonon relaxation time and the magnetoelastic constant in the film, respectively, must be adjusted slightly in order to maintain the agreement with W. It is found that for the glass substrate the τ value is increased from $\approx 0.90 \times 10^{-10}$ to $\approx 1.00 \times 10^{-10}$ sec and the b value is decreased from $\approx 6.87 \times 10^7$ to $\approx 6.66 \times 10^7$ erg/cm^3.

It is not surprising that the method of W and the present treatment give essentially identical results in the case of the substrate-free film. In W the actual spin wave and phonon in the film are treated, whereas in the present paper the two magnetoelastic waves, linear combinations of which yield the spin wave and the phonon, are dealt with. In fact, for the case when the spin-wave and phonon "skin depths" are much greater than the film thickness, it is possible to obtain from the

[1] R. Weber, Phys. Rev. **169**, 451 (1968).

[2] E. A. Turov and Yu. P. Irkhin, Phys. Metals Metallog. Res. (USSR) **3**, 15 (1956).

[3] C. Kittel, Phys. Rev. **110**, 836 (1958).

[4] A. I. Akhiezer, V. G. Bar'iakhtar, and S. V. Peletminskii, Zh. Eksperim. i Teor. Fiz. **35**, 228 (1958) [English transl.: Soviet Phys.—JETP **8**, 157 (1959)].

[5] E. Schlomann, J. Appl. Phys. **31**, 1647 (1960).

[6] H. E. Bömmel and K. Dransfeld, Phys. Rev. Letters **3**, 83 (1959).

[7] M. Pomerantz, Phys. Rev. Letters **7**, 312 (1961).

[8] M. F. Lewis, T. G. Phillips, and H. M. Rosenberg, Phys. Letters **1**, 198 (1962).

[9] M. H. Seavey, Jr., Trans. Ultrasonics Engr. UE-**10**, 49 (1963); and Proc. IEEE **53**, 1387 (1965).

[10] C. F. Kooi, Phys. Rev. **131**, 1070 (1963).

[11] P. Wigen, W. Dobrov, and M. Shanabarger, Phys. Rev. **140**, A1827 (1965).

[12] D. L. Mills, Phys. Rev. **157**, 369 (1967).

[13] This fact was in essence first pointed out in Ref. 7 and was discussed in detail for the inhomogeneous magnetization case in Ref. 12.

[14] This problem, for the case of a substrate-free film, was briefly treated earlier by the author in a Lincoln Laboratory Group Report, No. 82G-0029, 1961 (unpublished).

[15] V. A. Ignatchenko and E. V. Kuz'min, Zh. Eksperim. i Teor. Fiz. **49**, 787 (1965) [English transl.: Soviet Phys.—JETP **22**, 547 (1966)].

formulas presented here precisely the Eq. (5) of W for the field shift of the SWR. For the spin-wave and phonon relaxation times appropriate to the experimental case, it turns out that these "skin depths" are of the order of the film thickness. As a consequence of this, the resonance line is broadened somewhat, but the position of the peak is apparently not appreciably shifted. Such "skin depths" arise in the present treatment because it is a traveling-wave steady-state theory in which the frequency is taken as real and the wave numbers as complex.

The approach used here is similar to that of Ament and Rado[16]; that is, the system of coupled equations of motion is supplemented by Maxwell's equations for a good conductor and in the boundary-value problem use is made of the electromagnetic boundary conditions (continuity of tangential components of electric and magnetic fields). For the conductivity value chosen it turns out that the electromagnetic content of the magnetoelastic waves is small. In other words, the region of magnetoelastic crossover is well isolated from the eddy-current exchange region. This fact makes it possible to decouple the electromagnetic boundary conditions from the spin-wave and phonon boundary conditions. This simplifies considerably the solution of the boundary-value problem.

It is also assumed in the boundary-value problem that the spins are completely pinned on the film surfaces. The basis for this assumption rests on the experimental observation[17] that the SWR peak positions fit the expected spin-wave dispersion relation, i.e., $\omega \propto k^2$. This means that the spin-wave modes are indeed trigonometric functions of position and hence that they require some form of surface spin pinning in order to be excited. It is recognized that the pinning may not in fact be complete, but complete pinning is nevertheless assumed in order to simplify the derivation.

The parameters appropriate to the experimental case of W treated here (his sample 2) are listed as follows[17]: magnetization $M = 1083$ Oe, exchange constant $A = 1.12 \times 10^{-6}$ erg/cm, gyromagnetic ratio $\gamma = 18.82 \times 10^6$ rad/sec Oe, sound velocity (transverse) in the film $c_t = 3.10 \times 10^5$ cm/sec, density of film $\rho = 8.40$ g/cm³, composition of film is 70–30 permalloy, temperature of experiment is 77°K, thickness of film $d = 6170$ Å, half SWR linewidth $1/\gamma T = 85$ Oe, SWR order number $p = 23$, crossover frequency (consistent with $\omega = c_t k$, where $k = p\pi/d$) $f = 57.8$ GHz, difference between maximum and minimum magnetic field deviation on SWR tuning curve $\delta H_{mx} = 88.5$ Oe, frequency width between maximum and minimum magnetic field deviation $\delta f = 3.52$ GHz, and finally we have chosen a conductivity $\sigma = 1.6 \times 10^5$ mho/cm, which gives a skin depth $\delta \approx 5 \times 10^{-5}$ cm at 57.8 GHz.

In Sec. I, the general dispersion relation for the coupled electromagnetic, spin-wave, and acoustic

modes is described; the effect of damping on the shape of the dispersion curves is discussed. The solution of the boundary-value problem is described in Sec. II and the power absorption formulas are presented. In Sec. III the numerical results are discussed; also given is a discussion in terms of the dispersion diagram of how the SWR tuning curve arises.

I. PROPAGATION CONSTANTS

A. General Dispersion Relation and Eddy-Current Exchange Effect

This section begins with a discussion of the general dispersion relation for the coupled electromagnetic, spin-wave, and acoustic modes. The modes are circularly polarized in a plane perpendicular to the z direction, the direction of the dc magnetic field and the film normal, and rotate in the sense which produces resonance. When $\exp j(\omega t - kz)$ dependence is assumed, where ω is real and k complex, a simultaneous solution of Maxwell's equations, the equation of motion of the magnetization, and the appropriate acoustic wave equation yields the following relation:

$$\frac{2A}{M}(k^2 - k_m^2) - \frac{b^2 k^2}{\rho M c_t^2 (k^2 - k_e^2)} + \frac{4\pi M}{(1 - \frac{1}{2}j\delta^2 k^2)} = 0, \quad (1)$$

where

$$k_m^2 = (M/2A)(\omega/\gamma - H_i - j(1/\gamma T))$$

and

$$k_e^2 = (\omega^2/c_t^2)(1 - j(2/\omega\tau)).$$

Here b is the appropriate magnetoelastic constant for the film (B_2 in a cubic crystal), $H_i = H_a - 4\pi M$ is the internal magnetic field and H_a is the applied magnetic field, T is the phenomenological spin-wave relaxation time (for Landau-Lifshitz damping $1/\gamma T$ is replaced by $\lambda H_i/\gamma M$, where λ is the Landau-Lifshitz relaxation frequency), and τ is a phenomenological phonon relaxation time.

Equation (1) is a cubic equation in k^2. In the appropriate magnetic field or frequency regions the three solutions will correspond to predominantly electromagnetic, spin-wave, and acoustic modes. For the situation in the W experiment there are two magnetic field regions in which Eq. (1) reduces approximately to the product of a quadratic and a linear equation in k^2. These regions are centered about $H_i = \omega/\gamma$ and $H_i = \omega/\gamma - 2A\omega^2/Mc_t^2$ and correspond to the eddy-current exchange region and the magnetoelastic region, respectively. In the eddy-current exchange region, Eq. (1), becomes approximately

$$(k^2 - k_m^2)(k^2 + 2j/\delta^2) + j(4\pi M^2/A\delta^2) = 0, \quad (2a)$$

$$k^2 - k_e^2 = 0, \quad (2b)$$

while in the magnetoelastic region Eq. (1) becomes

[16] W. S. Ament and G. T. Rado, Phys. Rev. **97**, 1558 (1955).
[17] R. Weber (private communication).
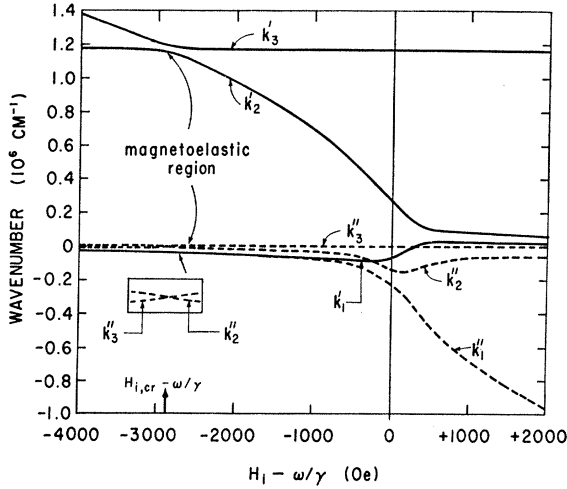
FIG. 1. Real and imaginary parts of the propagation constants versus magnetic field for the magnetoelastic waves $(k_2=k_2'+ik_2''$ and $k_3=k_3'+ik_3'')$ and for the electromagnetic mode $(k_1=k_1'+ik_1'')$. The figure shows that in terms of magnetic field the magnetoelastic region is well separated from the eddy-current exchange region. The curves are drawn to scale for the following parameters: $f=57.8$ GHz, $\sigma=1.6\times10^5$ mho/cm, $b\approx6.7\times10^7$ erg/cm^3, $1/\gamma T=85$ Oe, and $\tau\to\infty$.

approximately

$$(k^2-k_m{}^2)(k^2-k_e{}^2)-a^2k^2=0, \qquad (3a)$$

$$k^2+(2j/\delta^2)\mu=0, \qquad (3b)$$

where

$$a^2=b^2/2A\rho c_t{}^2$$

and

$$\mu=1-4\pi M/(\omega/\gamma-H_i-j(1/\gamma T)).$$

It is shown in the Appendix how Eqs. (2) and (3) are obtained from Eq. (1). It is clear from Eq. (2) that in the eddy-current exchange region the electromagnetic and spin-wave modes are admixed while the acoustic mode is uncoupled. From Eq. (3) we see that in the magnetoelastic region the spin-wave and acoustic modes are admixed while the electromagnetic mode is uncoupled.

Figure 1 is a plot drawn to scale of the real and imaginary parts of the wave numbers versus $H_i-\omega/\gamma$ for the case of the W experiment. The plot was obtained by using Eqs. (2) and (3), separately. It was found as expected on the scale used that the separate numerical solutions joined smoothly in the neighborhood of $H_i-\omega/\gamma\approx-2000$ Oe, that is, approximately midway between the magnetoelastic and eddy-current exchange regions. For convenience in plotting, an infinite value of τ was taken. This was done only to show the separation of k_2'' and k_3'' in the magnetoelastic region. In the experimental case the spin-wave and acoustic dampings are more nearly comparable. Figure 2 shows the $\omega/2\pi$-versus-k dispersion diagram also drawn to scale for the case of the W experiment and for $\tau\to\infty$. The curves are essentially unchanged on the scale used when the experimental τ value is taken.

The shape of the curves in the eddy-current exchange

region in Figs. 1 and 2 does not qualitatively change with increasing skin depth until the following condition, which can be obtained from Eq. (2a), holds:

$$|1/\gamma T-4A/M\delta^2|>\{32\pi A/\delta^2\}^{1/2}. \qquad (4)$$

(The right-hand side of this expression has the value 210 Oe.) If (4) is satisfied, branches 1 and 2 of the dispersion relation no longer "repel" each other in the neighborhood of $H_i=\omega/\gamma$. Instead, the branches cross and begin to resemble the nearly pure modes which are obtained from Eq. (2a) if the coupling term $j4\pi M^2/A\delta^2$ is made very small. A similar branch crossing for large damping also occurs for branches 2 and 3 in the magnetoelastic region and will be discussed in Sec. IB.

Let us examine under what conditions a possible overlap of the eddy-current exchange region and the magnetoelastic region may occur.[18] It is seen from Eq. (A3) of the Appendix that the eddy-current exchange contribution to the spin-wave damping, $1/\gamma T$, is given approximately by $16\pi A/\delta^2(\omega/\gamma-H_i)$. At the crossover field for the $p=23$ resonance $(\omega/\gamma-H_{i,\mathrm{cr}}=2840$ Oe) this contribution is 8 Oe, an order of magnitude less than $1/\gamma T$. It should be pointed out, however, that the σ value chosen is only an estimate based on the room-temperature value of 0.71×10^5 mho/cm for 70–30 permalloy.[19] (The W experiments were carried out at 77°K.) It is clear that if a somewhat larger value of σ
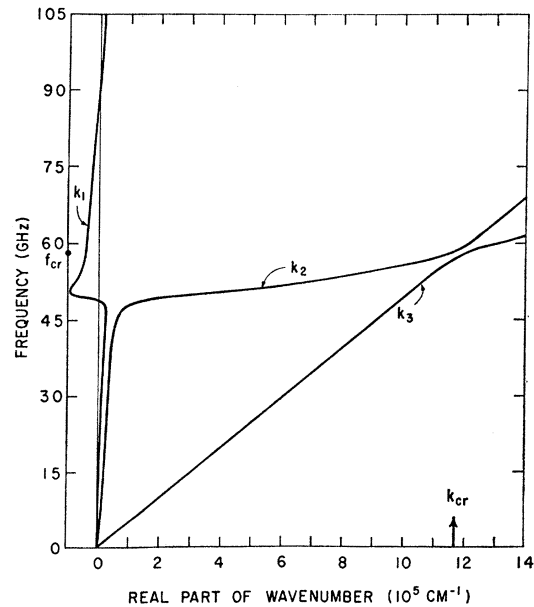
FIG. 2. General dispersion curve for the magnetoelastic waves $(k_2$ and $k_3)$ in the presence of an electromagnetic mode (k_1). Propagation is in the direction of the internal dc magnetic field. The curves are drawn to scale for $f_{\mathrm{cr}}=57.8$ GHz, $\sigma=1.6\times10^5$ mho/cm, $b\approx6.7\times10^7$ erg/cm^3, $1/\gamma T=85$ Oe, $\tau\to\infty$, and $H_i=H_{i,\mathrm{cr}}\approx16\,500$ Oe. The diagram shows that for the frequency of the W experiment the magnetoelastic region is well separated in k space from the eddy-current exchange region.

[18] The effect of conductivity on the damping of magnetoelastic waves has also been discussed in Refs. 2 and 3.
[19] R. M. Bozorth, *Ferromagnetism* (D. Van Nostrand Co., Princeton, N.J., 1951), p. 108.

than 1.6×10^5 mho/cm had been chosen, the eddy-current exchange-damping contribution would make up an appreciable fraction of the SWR linewidth in the magnetoelastic region. Since the exchange contribution is proportional to $(\omega/\gamma-H_i)^{-1}$, a narrowing of the linewidth with increasing SWR order number would then be observed.[20] The fact that the observed linewidths are essentially independent of order number[17] over a considerable region surrounding $p=23$ may be an indication that the value of σ chosen has not been greatly underestimated. At the lower microwave frequencies the magnetoelastic region begins to merge with the eddy-current exchange region and the situation in general becomes considerably more complex. It is assumed in this paper that the regions are well separated and that the electromagnetic content of the magnetoelastic waves is small.

B. Magnetoelastic Waves

When Eq. (3a) is solved for the propagation constant k the result is

$$k_2=\{(M/4A)[(\bar{H}+\bar{H}_{cr}+\bar{H}_{me})-i(1/\gamma T+1/\gamma\tau')$$
$$+(Y'+iY'')^{1/2}]\}^{1/2},\quad(5a)$$

$$k_3=\{(M/4A)[(\bar{H}+\bar{H}_{cr}+\bar{H}_{me})-i(1/\gamma T+1/\gamma\tau')$$
$$-(Y'+iY'')^{1/2}]\}^{1/2},\quad(5b)$$

where

$$Y'=(\bar{H}+\bar{H}_{me}-\bar{H}_{cr})^2-(1/\gamma T-1/\gamma\tau')^2+4\bar{H}_{me}\bar{H}_{cr},$$

$$Y''=-2(1/\gamma T-1/\gamma\tau')(\bar{H}+\bar{H}_{me}-\bar{H}_{cr})-4\bar{H}_{me}(1/\gamma\tau'),$$

and

$$\tau'=\tau(\omega/2\gamma\bar{H}_{cr}),\quad \bar{H}_{me}=2Aa^2/M=b^2/M\rho c_t^2,$$

$$\bar{H}_{cr}=2A\omega^2/Mc_t^2,\quad \bar{H}=(\omega/\gamma-H_i),$$

$$k_{2,3}=k_{2,3}'+k_{2,3}''.$$

The real and imaginary parts of the propagation constants k_2 and k_3 for $b=6.66\times10^7$ erg/cm³ and $\tau\rightarrow\infty$ are plotted versus magnetic field in Figs. 3(a) and 3(b). The figures illustrate the effect of increasing the spin-wave damping in the absence of acoustic damping. A similar qualitative change in the curves would occur if the acoustic damping were increased for zero spin-wave damping.[21] It may be noticed that curves d and e of Fig. 3(a) simply cross one another: There is no magnetoelastic gap in this case. It can be shown by examining the square root of $Y=Y'+iY''$ on the complex plane that a gap does not exist if the following condition is satisfied:

$$|1/\gamma T-1/\gamma\tau'|>(2A/M)\{2a(\omega/c_t)\}.\quad(6)$$

For $b=6.66\times10^7$ erg/cm³ the right-hand side of this inequality has the value 240 Oe at 57.8 GHz. Thus the condition is well satisfied for the curves e of Figs. 3(a)

[20] P. Pincus, Phys. Rev. **118**, 658 (1960). Such a narrowing was anticipated earlier in Ref. 16.
[21] This has been shown by R. Weber (see Ref. 17) for the case of nonzero spin-wave damping.
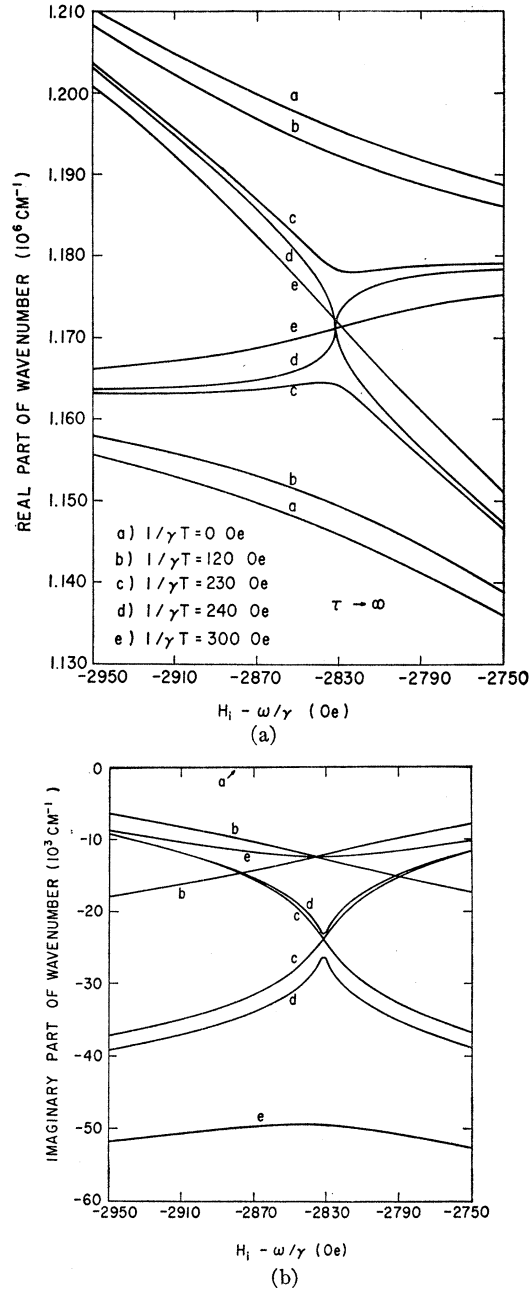
FIG. 3. Wave-number-versus-magnetic-field curves in the magnetoelastic region for $b=6.66\times10^7$ erg/cm³, $\tau\Rightarrow\infty$, and for the various values of the spin-wave damping, $1/\gamma T$, given in (a). (a) Real part of wave numbers. The magnetoelastic gap is not present in curves d and e. (b) Imaginary part of wave number. The curves for the experimental case lie between curves a and b.

and 3(b). Curves d of Figs. 3(a) and 3(b) apparently just satisfy condition (6). The curves for the experimental case ($b=6.66\times10^7$ erg/cm³, $\tau=1.00\times10^{-10}$ sec, and $1/\gamma T=85$ Oe) are not shown but lie between curves a and b on Figs. 3(a) and 3(b). Thus the condition (6) is clearly not satisfied in the experimental case.

Condition (6) lends itself to a simple physical interpretation. If the condition is multiplied on each side by γ, it can be shown by using Eq. (5) that the right-hand
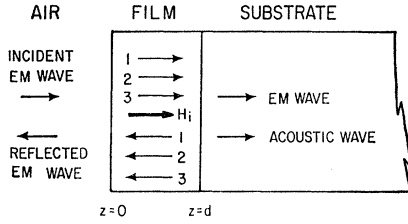
FIG. 4. Geometry of boundary-value problem.

side is equal to the minimum frequency splitting of the two branches in the absence of damping. Now if the term $1/\tau'$ is viewed as a kind of effective acoustic relaxation frequency, condition (6) states that if the *difference* in effective relaxation frequencies of the uncoupled spin-wave and acoustic modes exceeds the minimum frequency separation of the branches then the magnetoelastic gap is "washed out." If, however, both modes are heavily damped but have comparable dampings, the condition (6) states that the gap is still present. If the dampings become so large that the real and imaginary parts of each propagation constant become comparable then critically damped and uncoupled waves exist; but the discussion here is confined only to the case where the imaginary part of each propagation constant is much less than its real part. The latter is readily seen by comparing the ordinate scales of Figs. 3(a) and 3(b).

It is also interesting to note the behavior of the damping of the magnetoelastic modes with magnetic field. For the curves d and e in Fig. 3(b) the condition (6) is satisfied and this is why the curves do not intersect: the predominantly acoustic mode (upper curve d or e) attains its maximum spin-wave loading at the nominal crossover point but everywhere retains its identity as essentially an acoustic wave, while the predominantly spin-wave mode (lower curve d or e) has its loss reduced to a minimum at the nominal crossover while everywhere retaining its essentially spin-wave identity. The situation is changed when condition (6) is not satisfied. As shown by curves b and c in Fig. 3(b) the dampings exchange roles as we move through the crossover region (this is also seen in the inset in Fig. 1): the phononlike damping changes continuously into a spin-wave-like damping and vice versa. This behavior is of course a reflection of the fact that the magnetoelastic gap forces the phonon to change continuously into a spin wave and vice versa as the magnetic field is tuned through crossover.

It is important to note that in the experimental case the effective dampings are comparable. If we take $\tau = 1.00 \times 10^{-10}$ sec and use the definition of τ' given under Eq. (5), we obtain $\tau' = 3.3 \times 10^{-10}$ sec and $1/\gamma\tau' = 158$ Oe. This value of $1/\gamma\tau'$ is not far from the spin-wave damping value $1/\gamma T = 85$ Oe. It is seen that the damping difference, 73 Oe, is less than 240 Oe, the value which causes the gap to disappear. As mentioned above, the computed results for the propagation constants show that the magnetoelastic gap for these

values of τ and $1/\gamma T$ corresponds to a gap that lies between that determined by curves a and b of Fig. 3(a).

II. BOUNDARY-VALUE PROBLEM

The geometry of the problem is illustrated in Fig. 4.[22] A linear polarized electromagnetic wave is incident normally on the film from the air region on the left. Six modes, three for propagation in the $+z$ direction and three for the $-z$ direction, are shown in the film. These are all circularly polarized in the sense to produce resonance and have propagation constants equal to the plus and minus square roots of the three k^2 solutions of Eq. (1). The six oppositely rotating modes, which strictly speaking must also be present since the incident wave is linearly polarized, are neglected because their nonresonant character means that they are never excited to any appreciable level in the film, and furthermore there is no magnetoelastic crossover for these modes. There are two modes in the substrate, a circular polarized acoustic wave and an electromagnetic wave. The substrates used in W were glass, and hence any return acoustic wave from the far side of the substrate will be highly damped at the frequency of the experiment and is neglected here. For convenience any return electromagnetic wave is also neglected.

Each of the microwave quantities, i.e., the magnetic field h, the electric field e, the magnetization m, and the elastic displacement u, can be represented by a linear combination of the six normal modes in the film. For example, the magnetic field is given by

$$h = \sum_{i=1}^{3} h_i{}^{+} e^{-jk_i z} + \sum_{i=1}^{3} h_i{}^{-} e^{+jk_i z}. \tag{7}$$

The first summation here is over the $+z$-directed waves and the second over the $-z$-directed waves. The amplitudes $h_i{}^{\pm}$, $e_i{}^{\pm}$, $m_i{}^{\pm}$, and $u_i{}^{\pm}$ can be related for each i by "impedance" relations obtained from the coupled system of Maxwell's equations, the magnetization equation of motion, and the acoustic wave equation. There are thus six unknowns in the film. Outside the film on the air side there is one unknown, the reflected wave, and on the substrate side there are two unknowns, the transmitted electromagnetic wave and the acoustic wave amplitude. The nine boundary conditions required for these nine unknown quantities arise as follows: The requirement of continuity of tangential electric and magnetic field across the two film surfaces supplies four conditions; the assumption of spin pinning on each film surface supplies two more conditions; two conditions come from requirement of elastic stress continuity across the interfaces; and the final condition comes from the assumption of continuity of elastic displacement across the film-substrate interface.

---

[22] A very similar problem has been solved by V. A. Ignatchenko and E. V. Kuz'min, J. Appl. Phys. **39**, 494 (1968); and Fiz. Tverd. Tela (to be published). They obtain expressions for the acoustic power transmitted into the substrate and the electromagnetic power generated by a return acoustic wave from the far side of the substrate (single-crystal rod).

In principle the above described 9×9 system of equations can be solved for any of the field amplitudes in terms of the incident magnetic field amplitude. However, this is not necessary because it has been assumed that the electromagnetic content of the magnetoelastic waves is small. This means that in Eq. (7) the only terms which contribute appreciably are those in h_1^+ and h_1^-, the electromagnetic mode amplitudes. The four electromagnetic boundary conditions can thus be decoupled from the five conditions involving m and u. In the electromagnetic conditions the terms in $h_2^\pm$ and $h_3^\pm$ are neglected and the equations are solved for h_1^+, h_1^-, and the reflected and transmitted magnetic field amplitudes (circular polarized). The expressions for h_1^+ and h_1^- are then substituted into the remaining 5×5 system. This system can be solved for any of the quantities h_2^+, h_2^-, h_3^+, h_3^-, or u_0, where u_0 is the acoustic wave amplitude in the substrate.

In order to simplify the algebraic manipulations it has been assumed that the skin depth is much greater than the film thickness. This means that it is permissible to set $h_1^+ = h_1^- = h$, where h is the circular polarized portion of the incident magnetic field amplitude. This is not strictly justified, of course, because the skin depth (≈ 5000 Å) and the film thickness (6170 Å) are comparable. Possibly as a result of this small skin depth, the experiment shows even and odd SWR peaks of about equal strengths in the neighborhood of the crossover region.[17,23] The simplified case that is done here predicts only odd modes. The more appropriate boundary-value problem,[24] the solution to which would contain both even and odd modes for the skin depth assumed here, could have been worked out, but it was felt that the main results of this paper would not have been greatly changed. It is unlikely that the SWR tuning curve which is obtained in Sec. III for the odd mode $p=23$ would change significantly in character if we were to treat a more appropriate boundary-value problem and study the $p=22$ mode, for example.[25]

The power absorption per unit area in the film is calculated from the following formula:

$$P = -\frac{\omega}{8\pi}\,\mathrm{Im}4\pi\int_0^d mh^*\,dz. \qquad (8)$$

This is, of course, the integral over the film thickness of the magnetic absorption per unit volume. In Eq. (8) h is a constant and m is given as follows:

$$m = m_2 + m_3, \qquad (9)$$

where

$$m_2 = m_2^+ e^{-jk_2z} + m_2^- e^{+jk_2z} \qquad (10a)$$

and

$$m_3 = m_3^+ e^{-jk_3z} + m_3^- e^{+jk_3z}. \qquad (10b)$$

The amplitudes $m_2^\pm$ and $m_3^\pm$ are obtained by solving the above-mentioned 5×5 system of equations. When Eqs. (9) and (10) are substituted into Eq. (8) the power absorption can be expressed as the sum of the absorption of modes 2 and 3. Thus it is possible to compute the power absorbed from each magnetoelastic wave in the film. Since the m_1 term in Eq. (9) has been omitted it is clear that the electromagnetic mode absorption is not being considered. However, this merely presents a slowly varying background and does not affect the SWR.

The expression for the power absorption which has been calculated by using Eq. (8) is now written down. The incident power is given as $P_0 = (c/8\pi)h^2$, where c is the velocity of light in vacua and h is the properly rotating circular polarized component of the incident linear-polarized magnetic field amplitude. The relative power absorption is

$$P/P_0 = P_2/P_0 + P_3/P_0, \qquad (11)$$

where

$$P_2/P_0 = 2(f/\sigma)^{1/2}(\mu_{R\ \mathrm{equ}\ 2})^{1/2} \qquad (12a)$$

and

$$P_3/P_0 = 2(f/\sigma)^{1/2}(\mu_{R\ \mathrm{equ}\ 3})^{1/2}. \qquad (12b)$$

The quantity $\mu_{R\ \mathrm{equ}}$ is proportional to the real part of the equivalent surface impedance.[16] One such quantity exists for each branch of the dispersion relation, i.e., for each magnetoelastic wave. The expressions for the square roots of these quantities are

$$(\mu_{R\ \mathrm{equ}\ 2})^{1/2} = \frac{8\pi M}{(\omega/\gamma - H_i)\delta}\,\mathrm{Re}\left[\frac{k_3^2(k_e^2 - k_2^2)\zeta_3 k_e^{-2}k_2^{-1}\tanh\frac{1}{2}jk_2d + \frac{1}{4}ra^2(k_2^2 + k_3^2)k_e^{-1}(k_3^2 - k_2^2)^{-1}}{k_3^2 - k_2^2 - ra^2(k_2k_e(k_2^2 - k_e^2)^{-1}\coth jk_2d - k_3k_e(k_3^2 - k_e^2)^{-1}\coth jk_3d)}\right], \qquad (13a)$$

$$(\mu_{R\ \mathrm{equ}\ 3})^{1/2} = \frac{8\pi M}{(\omega/\gamma - H_i)\delta}\,\mathrm{Re}\left[\frac{k_2^2(k_3^2 - k_e^2)\zeta_2 k_e^{-2}k_3^{-1}\tanh\frac{1}{2}jk_3d + \frac{1}{4}ra^2(k_2^2 + k_3^2)k_e^{-1}(k_3^2 - k_2^2)^{-1}}{k_3^2 - k_2^2 - ra^2(k_2k_e(k_2^2 - k_e^2)^{-1}\coth jk_2d - k_3k_e(k_3^2 - k_e^2)^{-1}\coth jk_3d)}\right], \qquad (13b)$$

where

$$\zeta_2 = 1 + r\left\{\frac{k_3^2(k_2^2 - k_e^2) - [2k_e^2k_2^2 - k_3^2(k_2^2 + k_e^2)]\cosh jk_2d}{2k_2k_e(k_3^2 - k_2^2)\sinh jk_2d}\right\}$$

---

[23] Partial spin pinning at the surface may also be involved here.

[24] Since in the experiment the film is usually in electrical contact with the cavity wall (see Ref. 17), an even more appropriate boundary-value problem would be the case for which the incident electromagnetic wave enters from the substrate side.

[25] For a driving field amplitude that exponentially decays with z it is pointed out in W that the even mode resonance behaves similarly to the odd mode resonance in the crossover region.

and

$$\zeta_3 = 1 - r \left\{ \frac{k_2^2(k_3^2 - k_e^2) - [2k_e^2 k_3^2 - k_2^2(k_3^2 + k_e^2)] \cosh j k_3 d}{2k_3 k_e(k_3^2 - k_2^2) \sinh j k_3 d} \right\}.$$

Here k_2 and k_3 are obtained from Eq. (5), k_e^2 is given under Eq. (1), and a^2 is defined under Eq. (3). The quantity r is a complex acoustic impedance ratio and is given by

$$r = \frac{Z_s}{Z_f}\left(\frac{1 - i/\omega\tau_s}{1 - i/\omega\tau_f}\right), \qquad (14)$$

where $Z = \rho c_t$ is the acoustic impedance, the subscript s refers to the substrate, and the subscript f refers to the film.

An expression for the acoustic power transmitted into the substrate has also been derived. However, as is described in Sec. III, the results of computer calculations based on this expression show that this power is usually small compared to the absorption in the film. Hence the expression is not given here.

III. NUMERICAL RESULTS

A. Substrate-Free Case

In order to compare the results of the present paper with those of W, the case of $r=0$ in Eq. (13) is first treated, i.e., the case of the substrate-free film. It is of interest to compute the shift of the SWR peak position with frequency, as this is the important experimentally determined quantity. This shift is given by

$$\delta H_p = H_p - [\omega/\gamma - (2A/M)k_p^2], \qquad (15)$$

where H_p is the SWR magnetic field position and $[\omega/\gamma - (2A/M)k_p^2]$ is its position in the absence of magnetoelastic effects (i.e., for $b=0$). The SWR order number p is 23, $k_p = p\pi/d$, and the fields are internal, i.e., applied field minus $4\pi M$. The resonance line for $p=23$ is computed for a particular frequency by using Eqs. (11)-(13) and the magnetic field of the resonance peak is noted. This has been done over a range of frequencies using the AFCRL 7044/7094 computer facility. Figure 5 is a plot of $H_{23} - \omega/\gamma$ versus frequency for $\tau = 0.903 \times 10^{-10}$ sec and $b = 6.87 \times 10^7$ erg/cm^3. These values of b and τ were computed from the experimentally observed[17] values $\delta f = (1/2\pi)\delta\omega = 3.52$ GHz and $\delta H_{mx} = 88.5$ Oe by using the following expressions:

$$\delta\omega = 2/\tau, \qquad (16)$$

$$\delta H_{mx} = \tau b^2 k_p / 2\rho c_t M. \qquad (17)$$

These expressions can be obtained by differentiating Eq. (5) of W. Note that the curve of Fig. 5 gives $\delta f = 3.46$ GHz and $\delta H_{mx} = 92.3$ Oe. This proves that the theory presented here is in quite good agreement with that given in W for the case of the substrate-free film. It can also be shown that the wings of the curve of Fig. 5 agree well with the theoretical result of W, i.e., with the prediction of his Eq. (5). The experimental points

fall off this curve rapidly on the wings beyond the maximum and minimum points. This is described by W. The reason for this behavior is not clear, but is briefly speculated upon at the end of the paper.

Plots of relative power absorption versus magnetic field are given in Fig. 6 for $r=0$, $\tau=0.903\times10^{-10}$ sec, and $b=6.87\times10^7$ erg/cm^3. Almost identical power absorption plots are obtained for $r=0.35$ (appropriate to a glass substrate) if $\tau=1.00\times10^{-10}$ sec and $b=6.66\times10^7$ erg/cm^3. The separate power absorptions for each magnetoelastic wave and the total absorptions which are their sums are shown. Above the absorption curves for each part of Fig. 6 are shown the dispersion curves for the magnetoelastic waves. A study of these figures will show how the SWR tuning curve of Fig. 5 arises.[26]

Each magnetoelastic wave must be considered from the point of view of the rf magnetic field. For example, in Fig. 6(a) the rf field can interact strongly with the upper branch mode (k_3) near the $H_i - \omega/\gamma = -3350$ Oe end of the curve, since at this end the field sees the mode essentially as a spin wave. At the other end of the branch, where the mode is essentially a phonon, the spin-wave "handle" for the rf field is very weak indeed. It is thus reasonable that the absorption peak for the mode should fall to the left (low-field side) of the circled point on the branch: Competition exists as the magnetic field increases, between the decreasing spin-
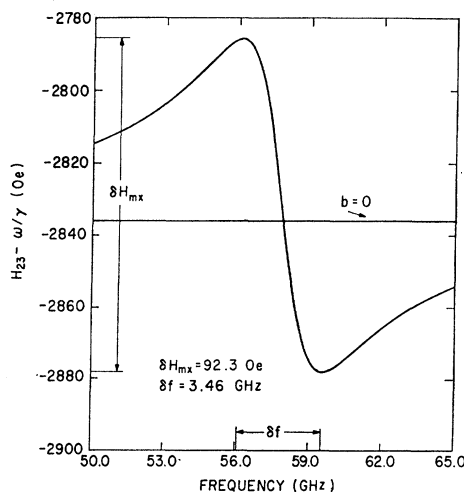
FIG. 5. Computed resonance field for the $p=23$ SWR as a function of frequency for the case of zero substrate impedance. The values of b and τ used in the computation were 6.87×10^7 erg/cm^3 and 0.903×10^{-10} sec, respectively, and were calculated from Eqs. (15) and (16) of the text by using the experimental values $\delta f = 3.52$ GHz and $\delta H_{mx} = 88.5$ Oe.

[26] The present discussion of the SWR tuning curve differs from that given in W in that here reference is made specifically to power absorption curves for each magnetoelastic wave as a function of magnetic field.
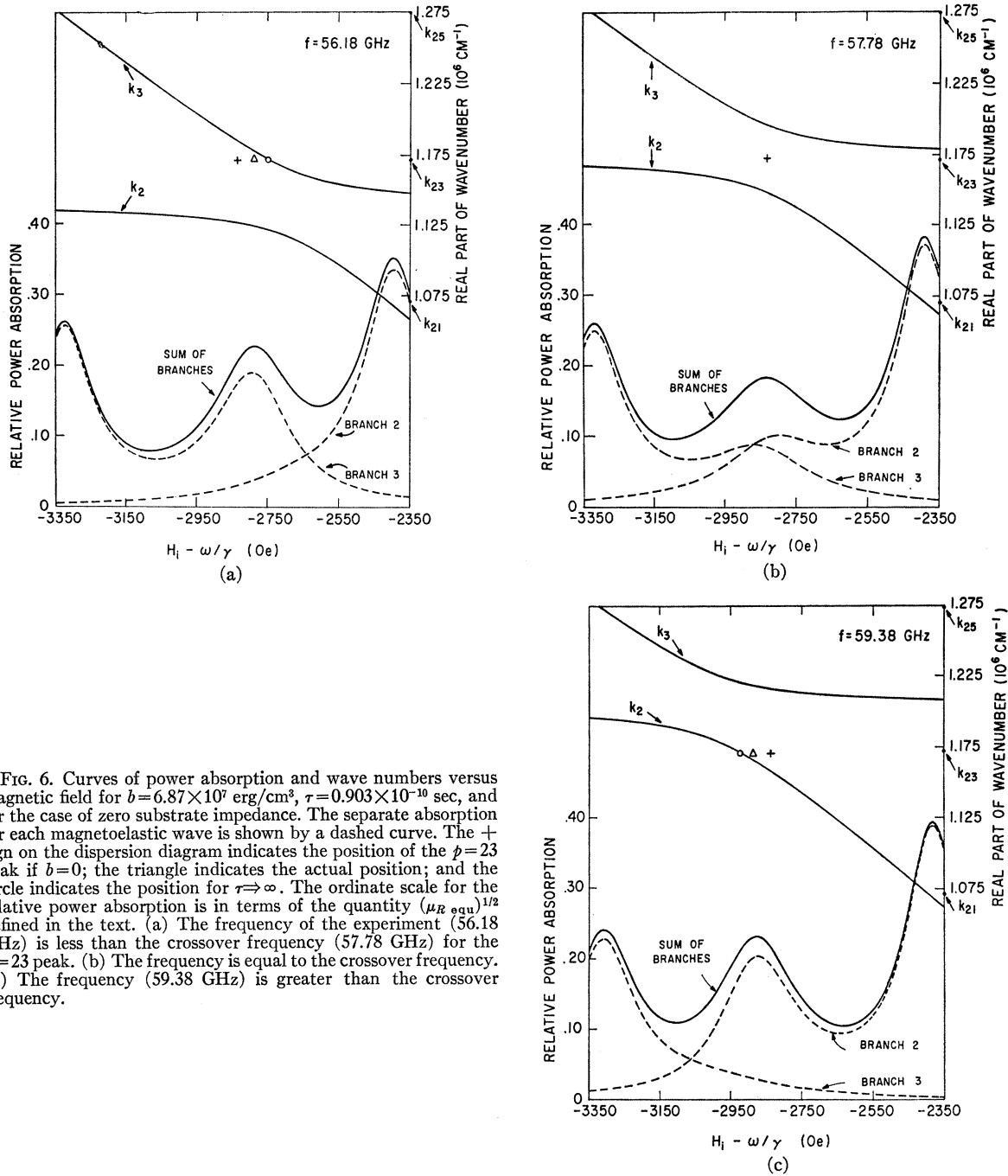
FIG. 6. Curves of power absorption and wave numbers versus magnetic field for $b=6.87\times10^7$ erg/cm^3, $\tau=0.903\times10^{-10}$ sec, and for the case of zero substrate impedance. The separate absorption for each magnetoelastic wave is shown by a dashed curve. The $+$ sign on the dispersion diagram indicates the position of the $p=23$ peak if $b=0$; the triangle indicates the actual position; and the circle indicates the position for $\tau\Rightarrow\infty$. The ordinate scale for the relative power absorption is in terms of the quantity $(\mu_{R\ \mathrm{equ}})^{1/2}$ defined in the text. (a) The frequency of the experiment (56.18 GHz) is less than the crossover frequency (57.78 GHz) for the $p=23$ peak. (b) The frequency is equal to the crossover frequency. (c) The frequency (59.38 GHz) is greater than the crossover frequency.

wave content of the mode and the increasing tendency of the mode to satisfy the SWR condition. In Fig. 6(b) the frequency has been increased from that in Fig. 6(a) and now is equal to the crossover frequency for the SWR. The total absorption peak (sum of the branches) falls essentially at the $b=0$ magnetic field position. This is because the separate magnetoelastic wave absorption peaks occur at k numbers that are symmetrically spaced about k_{23}. The spin-wave content of the modes at these k numbers apparently has its optimum value from the point of view of the rf driving

field. Figure 6(c), for which the frequency has been further increased, shows the SWR occurring to the right of the circled place on the lower branch (k_2). This happens for reasons analogous to those for Fig. 6(a). Thus it is seen that the SWR peak position must move first to higher fields and then to fields lower than the $b=0$ field position as the frequency is increased through crossover. On the wings of the SWR tuning curve the k numbers corresponding to the peak positions have returned almost completely to the respective branches of the dispersion relation. It is in the region of
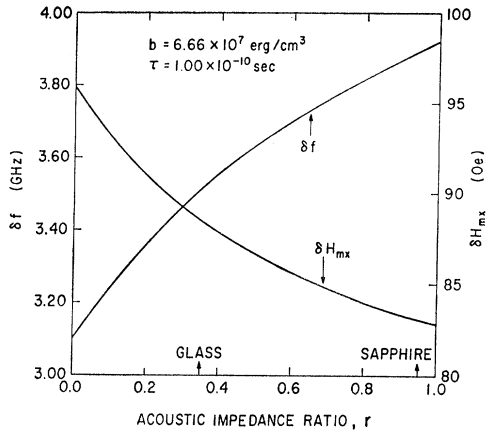
FIG. 7. Curves of δf and δH_{mx} versus substrate to film acoustic impedance ratio for $b=6.66\times10^7$ erg/cm^3 and $\tau=1.00\times10^{-10}$ sec. These values of b and τ give the experimentally observed values $\delta f=3.52$ GHz and $\delta H_{mx}=88.5$ Oe for a glass substrate $(r=0.35)$.

the wings, however, as was stated earlier, where the experimental points fall away rapidly from their predicted values and approach their $b=0$ positions more quickly than expected.

The over-all shape of the SWR tuning curve is very sensitive to the independent acoustic damping mechanism (expressed in τ). In fact it is seen from Eqs. (16) and (17) that the inverse frequency width and the magnetic field height of the curve are directly proportional to τ. This damping mechanism is all important in the competing process between the spin-wave content of a mode and its tendency to satisfy the SWR condition. For example, in Fig. 6(a), if the acoustic damping were absent $(\tau\Longrightarrow\infty)$ the rf field could still interact with the upper branch mode at the extreme high field end: the spin-wave content of the mode would be very small, but in compensation for this the mode would be essentially undamped. Thus it is reasonable to expect for increasing τ that the triangle marking the absorption peak in Fig. 6(a) moves back toward the circle. This process should be independent of the separate spin-wave damping mechanism (expressed in T). In Fig. 6(b) if we let $\tau\Longrightarrow\infty$ the rf field could interact with the modes far out onto the wings of the dispersion curve. The SWR line for $p=23$ would then be expected to disappear. This has in fact been verified by the appropriate computer calculations.

There is a simpler viewpoint of course from which to consider the SWR tuning curve. This is the coupled resonance circuit analogy in which an acoustic resonator is considered as a load on the resonant circuit for the spin wave.[27] At the crossover frequency for the SWR the acoustic loading becomes purely resistive. This is

---

[27] Coupled transmission line models of magnon-phonon modes in ferrites have been worked out by J. Sethares, Air Force Cambridge Research Laboratory Physical Science Research Paper No. 327, 1967 (unpublished); and IEEE, PGUE (to be published).

seen from the fact that in Fig. 6(b) the peak occurs at the $b=0$ position and the broadening of the resonance line is greatest. At frequencies to either side of crossover the acoustic loading becomes partly reactive and a 180° phase shift in the loading occurs as the frequency is changed through crossover. For $\tau\Longrightarrow\infty$ the acoustic system is no longer independently damped and "shorts out" the SWR at crossover.

It is difficult to compare the resonance linewidths shown in Fig. 6 with experiment. This is because the experimental lines are a combination of Gaussian and Lorentzian,[17] whereas the lines of Fig. 6 are essentially Lorentzian and are somewhat merged together. If, however, an arbitrary base line at approximately the minimum absorption points is taken, it is found that a linewidth increase of about 60% in going to crossover ($\frac{1}{2}\Delta H\cong70$ Oe off crossover and 110 Oe on crossover) occurs. The experimental increase is about 20% ($\frac{1}{2}\Delta H=85$ Oe off crossover and 100 Oe on crossover).[17] If a zero base line is taken in Fig. 6 the half-widths far from crossover are about 100 Oe. The fact that the spin-wave "skin depth" is of the order of the film thickness is probably responsible for this slight increase over the expected value of $\frac{1}{2}\Delta H=1/\gamma T=85$ Oe.

B. Case of Film Attached to Substrate

As the acoustic impedance of the substrate is increased from zero it is reasonable to expect that an additional loading is placed on the acoustic system in the film. This loading produces a weakening of the observed magnon-phonon interaction in the film. This may be seen as follows: Assume first that the substrate impedance is very large compared to the film impedance. Then the acoustic wave is essentially pinned at the interface. Physically, the pinning makes the film an odd-integer *quarter-wave*-type acoustic resonator since the air-film interface is assumed to be a free surface acoustically. However, the film is an odd-integer *half-wave*-type spin-wave resonator, and hence it is not strictly possible to satisfy the magnon-phonon matching condition. If the substrate impedance is not very large compared to the film impedance, this detuning of the magnon-phonon resonance is of course somewhat less but is still present. In addition to this detuning effect a nonzero but finite substrate impedance means that acoustic power is radiated into the substrate. Computer results have shown, however, that for the case of the W experiment this power loss is small compared to the SWR absorption even under acoustic match conditions. This small power loss, when added to the SWR absorption, does not significantly change the magnetic field position of the SWR.

It was mentioned in Sec. IVA above that power absorption curves almost identical to those in Fig. 6 were obtained for $r=0.35$ by taking $\tau=1.00\times10^{-10}$ sec and $b=6.66\times10^7$ erg/cm^3. These values of τ and b were found by a computer search to locate those unique

values of τ and b which yield the experimental values $\delta f = 3.52$ GHz and $\delta H_{\mathrm{mx}} = 88.5$ Oe for $r = 0.35$. The value of $r = 0.35$ was determined by taking $\rho = 2.20$ g/cm^3 and $c_t = 4.1 \times 10^5$ cm/sec for glass,[28] the substrate material used in the W experiment. Thus the substrate impedance is $Z_s = \rho c_t = 9.0 \times 10^5$ g/cm^2 sec and since the film impedance $Z_f = 26.0 \times 10^5$ g/cm^2 sec, the result is $r = Z_s/Z_f = 0.35$. It is assumed that in Eq. (14) both $\omega \tau_s$ and $\omega \tau_f$ are much greater than unity.

In Fig. 7 curves are presented of δf and δH_{mx} versus the acoustic impedance ratio r for $\tau = 1.00 \times 10^{-10}$ sec and $b = 6.66 \times 10^7$ erg/cm^3. It is seen that the width of the interaction, δf, increases while the magnitude δH_{mx} decreases with increasing r. Thus, as expected, formulas (11)–(13) predict a weakening of the magnon-phonon interaction in the film in the presence of the acoustic loading by the substrate. In the present case, the rate of change of δf and δH_{mx} with r is a strong function of the intrinsic acoustic relaxation time of the film. This is because for $\tau \approx 1 \times 10^{-10}$ sec the phonon mean free path is 3100 Å or about one-half the film thickness. For longer mean free paths it is reasonable to expect that the acoustic loading effect of the substrate will be increased and become independent of τ for free paths much greater than the film thickness. Computer results based on formulas (11)–(13) have shown that for $\tau \gtrsim 3 \times 10^{-10}$ sec the interaction in the immediate neighborhood of the crossover frequency is entirely tuned out for $r \gtrsim \approx 1$; i.e., in the SWR tuning curve such as shown in Fig. 5, a central flat portion nearly coincident with the $b = 0$ line appears. Figure 7 shows that in the present case if the substrate is changed from glass to sapphire ($Z_s \approx 25 \times 10^5$ g/cm^2 sec) the width of the interaction increases by about 10% and the height decreases by about 6%.

Finally, it is to be noted that for parameters appropriate to the W experiment the over-all shape of the SWR tuning curve is essentially independent of the value of substrate impedance chosen. Thus, the presence of the substrate impedance does not cause a lowering of the wings of the curve in the direction of the experimental points. It appears likely that a one-dimensional monochromatic plane-wave theory is not adequate to describe the SWR tuning curve in the region of its wings. If inhomogeneous broadening of the magnon-phonon interaction were present, this could help to explain at least part of the observed rapid convergence in the wings of the curve. An obvious "inhomogeneity" is the finite thickness of the film. The finite thickness causes a spread of wave numbers over a region of k space of the order of $2\pi/d$. For $d = 6170$ Å the corresponding frequency interval around crossover is 0.15 GHz. This is small compared to the 3.52-GHz width of the SWR tuning curve. Additional inhomogeneities, however, may be caused by the presence of crystallites

which are of the order of the acoustic wavelength (≈ 500 Å). Such crystallites constitute nonperiodic perturbations of spatial dimension well suited for producing the one-magnon–one-phonon scattering necessary for the inhomogeneous broadening.

ACKNOWLEDGMENT

APPENDIX

For the situation in the W experiment it is readily shown that Eq. (1) reduces approximately to Eq. (2) or (3) in the appropriate field region. First Eq. (1) is rearranged as follows:

$$(k^2 - k_{01}^2)(k^2 - k_{02}^2)(k^2 - k_{03}^2) = a^2 k^2 (k^2 + 2j/\delta^2), \quad \text{(A1)}$$

where k_{01}^2 and k_{02}^2 are the roots of Eq. (2a) and $k_{03}^2 = k_e^2$. For $\omega/\gamma - H_i \geq 1000$ Oe approximate solutions of Eq. (2a) are

$$k_{01}^2 = -\frac{2j}{\delta^2}\left[1 - \frac{4\pi M}{\omega/\gamma - H_i - j/\gamma T}\right], \quad \text{(A2)}$$

$$k_{02}^2 = \frac{M}{2A}\left[(\omega/\gamma - H_i) - j\left(1/\gamma T + \frac{16\pi A}{\delta^2(\omega/\gamma - H_i)}\right)\right]. \quad \text{(A3)}$$

Substitution of the appropriate numerical values (given in the Introduction) gives $|k_{01}^2| \leq 2 \times 10^{10}$ cm^{-2} and $|k_{02}^2| \geq 5 \times 10^{11}$ cm^{-2} for $\omega/\gamma - H_i \geq 1000$ Oe. Also, $|k_{03}^2| = |k_e^2| \approx 10^{12}$ cm^{-2} and $|2j/\delta^2| \approx 10^9$ cm^{-2}. For k values in the magnetoelastic region, i.e., for $k \approx k_e \approx 10^6$ cm^{-1}, $|k^2| \gg |k_{01}^2|$. Thus, it is clear that the first factor on the left-hand side of Eq. (A1) and the last factor on the right-hand side may be cancelled. The result is the magnetoelastic dispersion relation, Eq. (3a). Equation (3b) is expressed by $k^2 - k_{01}^2 = 0$, where k_{01}^2 is given by Eq. (A2). That this is a good approximation for $\omega/\gamma - H_i \geq 1000$ Oe may be seen by solving Eq. (A1) for $(k^2 - k_{01}^2)/k_{01}^2$. The result is given approximately by

$$\frac{k^2 - k_{01}^2}{k_{01}^2} = \frac{a^2(k_{01}^2 + 2j/\delta^2)}{k_{02}^2 k_{03}^2}.$$

Since $a^2 \approx 0.25 \times 10^{10}$ cm^{-2} for $b = 6.66 \times 10^7$ erg/cm^3, this gives $|(k^2 - k_{01}^2)/k_{01}^2| \approx 10^{-4}$. At magnetoelastic crossover $\omega/\gamma - H_i \approx 2840$ Oe and hence it is clear that Eq. (3) is a good approximation to Eq. (1) in the vicinity of the crossover region.

In the region around $H_i = \omega/\gamma$ it is anticipated that the spin-wave and electromagnetic k values are considerably less than in the magnetoelastic region. Taking $k \approx 10^5$ cm^{-1} it is computed that the left-hand side of Eq. (A1) has an absolute value of approximately

---

[28] W. P. Mason, *Physical Acoustics* (Academic Press Inc., New York, 1965), Vol. III—Part B, Chap. 2, p. 64.

10^{34} while the right-hand side is less than 10^{30}. In fact the right-hand side of Eq. (A1) can be neglected compared to the left-hand side until the k values are approximately 10^6 cm^{-1}. Thus in the vicinity of $H_i = \omega/\gamma$ Eq. (2a) is a valid approximation. For the acoustic

mode near $H_i = \omega/\gamma$, Eq. (A1) yields approximately

$$(k^2 - k_{03}{}^2)/k_{03}{}^2 = a^2/k_{03}{}^2.$$

Since $|a^2/k_{03}{}^2| \approx 0.25 \times 10^{-2}$, it is permissible to let $k^2 = k_{03}{}^2$ in the vicinity of $H_i = \omega/\gamma$. This gives Eq. (2b).

Effects of Impurities on Spin Fluctuations in Almost Ferromagnetic Metals

Peter Fulde

Institut Max von Laue-Paul Langevin, (8046) Garching bei München, Germany

AND

Alan Luther[*]

Max Planck Institut für Physik und Astrophysik, (8) München, Germany

(Received 4 December 1967)

We investigate the effects of the mean free path on the spin susceptibility of almost ferromagnetic metals. Using these results, we calculate the low-temperature specific-heat contribution of the spin fluctuations. While the term linear in temperature T is unaffected by the mean free path, we find that the $T^3 \ln T$ contribution is rapidly modified by impurities, in contrast to the phonon case.

I. INTRODUCTION

SPIN fluctuations in almost ferromagnetic fermion systems have recently received very much attention. Such systems have an appreciably enhanced static spin susceptibility, indicating that the exchange interaction is important but not quite strong enough to lead to a ferromagnetic instability. For example, it was shown by Berk and Schrieffer[1] that in metals like Pd spin fluctuations lead to a change in the effective mass and can suppress superconductivity. Furthermore, Doniach and Engelsberg[2] made the important observation that in liquid He^3 spin fluctuations are responsible for the deviations of the temperature dependence of the specific heat from a Sommerfeld law. In Ref. 1 as well as in Ref. 2 it was furthermore shown that one can calculate the self-energy of the electrons due to exchange scattering in a simple fashion by formally introducing a propagator[3] for the paramagnon or spin fluctuations. There are several common features between the self-energy due to paramagnons and the one due to phonons.

However, as we show here, these similarities hold only in the limit of infinite mean free path, which is the only case for which exchange-enhanced spin fluctuations have been studied up to now. Since scattering centers

are present in most physical situations, we want to study their influence on spin fluctuations in this communication. The physical consequences for such quantities as the electronic self-energy and the electronic specific heat are discussed.

Our aim is to study first how the paramagnon propagator changes if a mean free path due to scattering centers is introduced. This is done in the next section. It turns out that for momenta q such that $ql \ll 1$, where l is the electronic mean free path, the paramagnon propagator changes drastically and becomes one which is of the diffusion type. The calculations are done by a standard vertex renormalization procedure. In Sec. III, we show how this change in the paramagnon propagator for $ql \ll 1$ can influence various physical quantities by studying the specific heat and the effective mass due to spin fluctuations.

It is found that the effective mass at zero temperature and hence the term in the specific heat which is linear in T are practically independent of mean free path. The contribution to the specific heat which is of the form $T^3 \ln T$, however, is replaced by $T^3 \ln(T + T_{\text{imp}})$, where T_{imp} is of the order of the impurity scattering rate times a reciprocal susceptibility enhancement factor. Thus, at low temperatures, this correction term goes over into a T^3 law, which has the same temperature dependence as many other contributions. We contrast this situation to the phonon case, where the $T^3 \ln T$ contribution to the electronic specific heat is not sensitive to mean free path. A magnonlike contribution of the form $T^{3/2}$ is found for temperatures below T_{imp}, whose coefficient is proportional to the three-halves power of

---

[*] NATO Postdoctoral Fellow. On leave of absence from U.S. Naval Ordnance Laboratory, Silver Spring, Md.

[1] N. F. Berk and J. R. Schrieffer, Phys. Rev. Letter **17**, 433 (1966).

[2] S. Doniach and S. Engelsberg, Phys. Rev. Letters **17**, 750 (1966).

[3] We will use the terminology "propagator," despite the fact that paramagnons are not elementary excitations of the system, and note that this is permissible in the spirit of the RPA.